



## Selective antimicrobial activity and mode of action of adeptantins, glycine-rich peptide antibiotics based on anuran antimicrobial peptide sequences

Nada Ilić<sup>a</sup>, Mario Novković<sup>a</sup>, Filomena Guida<sup>b</sup>, Daniela Xhindoli<sup>b</sup>, Monica Benincasa<sup>b</sup>, Alessandro Tossi<sup>b</sup>, Davor Juretić<sup>a,\*</sup>

<sup>a</sup> Faculty of Science, University of Split, Nikole Tesle 12, 21000 Split, Croatia

<sup>b</sup> Department of Life Sciences, University of Trieste, Via Giorgieri 5, 34127 Trieste, Italy

### ARTICLE INFO

#### Article history:

Received 28 June 2012

Received in revised form 29 October 2012

Accepted 14 November 2012

Available online 27 November 2012

#### Keywords:

Antimicrobial peptide

Helical peptide

Membranolytic

Selectivity index

### ABSTRACT

A challenge when designing membrane-active peptide antibiotics with therapeutic potential is how to ensure a useful antibacterial activity whilst avoiding unacceptable cytotoxicity for host cells. Understanding their mode of interaction with membranes and the reasons underlying their ability to distinguish between bacterial and eukaryotic cytoplasmic cells is crucial for any rational attempt to improve this selectivity. We have approached this problem by analysing natural helical antimicrobial peptides of anuran origin, using a structure–activity database to determine an antimicrobial selectivity index (SI) relating the minimal inhibitory concentration against *Escherichia coli* to the haemolytic activity ( $SI = HC_{50}/MIC$ ). A parameter that correlated strongly with SI, derived from the lengthwise asymmetry of the peptides' hydrophobicity (sequence moment), was then used in the “Designer” algorithm to propose novel, highly selective peptides. Amongst these are the ‘adeptantins’, peptides rich in glycines and lysines that are highly selective for Gram-negative bacteria, have an exceptionally low haemolytic activity, and are less than 50% homologous to any other natural or synthetic antimicrobial peptide. In particular, they showed a very high SI for *E. coli* (up to 400) whilst maintaining an antimicrobial activity in the 0.5–4  $\mu M$  range. Experiments with monomeric, dimeric and fluorescently labelled versions of the adeptantins, using different bacterial strains, host cells and model membrane systems provided insight into their mechanism of action.

© 2012 Elsevier B.V. All rights reserved.

### 1. Introduction

New anti-infective agents with a reduced propensity for inducing bacterial resistance are increasingly sought after to combat infections by antibiotic resistant strains of bacteria [1]. Cationic antimicrobial peptides (AMPs) produced by all higher organisms are ancient components of innate immunity that have remained effective against bacteria throughout evolution [2,3]. For many of these peptides, the main targets of action are the bacterial membranes and associated biological functions [4]. Altering membrane features which favour interaction with cationic AMPs, such as its composition rich in anionic phospholipids or the strong, inside-directed electric field, is a costly process for bacteria and is limited in both extent and time [5]. Furthermore, endogenously produced AMPs tend to act on multiple targets in bacteria, and can also have important pro-defensive effects on host immune cells [6]. For all these reasons, AMPs have a relatively

low tendency to elicit resistance, and often display a significant selectivity for bacterial with respect to host cells.

Thousands of endogenous AMPs from a multitude of vertebrate and invertebrate animals, plants and moulds have been reported (for a comprehensive list of databases collecting their sequences see [7]). A particularly abundant and wide-spread type of AMP acquires an amphipathic  $\alpha$ -helical secondary structure in a membrane-like environment [8]. Generally, however, the primary or secondary structures of these peptides have not been defined by parameters that can be quantitatively related to antibacterial and cytotoxic activities. Even when such structural parameters are identified, altering them so as to optimize the antibacterial activity whilst simultaneously maintaining a low cytotoxicity, or reducing it, has been a considerable challenge. An optimal combination of specific attributes favouring an improved selectivity without losing activity is not easily achieved [9–12]. Rational design methods for improving this balance would benefit from the identification of inherent structural features of AMPs which have evolved to ensure, within their natural context, a selective action in fending off microbes without endangering host cells.

A simple parameter used to quantify selectivity of AMPs (antimicrobial selectivity index or SI) is defined as the ratio between the concentrations leading to 50% lysis of human erythrocytes and the minimum concentration inhibiting bacterial growth ( $SI = HC_{50}/MIC$ ), which is

**Abbreviations:** AMP, antimicrobial peptide; BODIPY, boron-dipyrromethene; Gal-ONp, o-nitrophenyl- $\beta$ -D-galactopyranoside;  $HC_{50}$ , concentration for 50% haemolysis;  $IC_{50}$ , concentration for 50% of growth inhibition; LUVs, large unilamellar vesicles; MIC, minimum inhibitory concentration; MBC, minimal bactericidal concentration; PI, propidium iodide; TFE, trifluoroethanol; SI, antimicrobial selectivity index

\* Corresponding author. Tel.: +385 21 385 133; fax: +385 21 384 086.

sometimes also indicated as a ‘therapeutic index’. We have collected the SI values derived from published  $HC_{50}$  and MIC (*Escherichia coli*) data for numerous anuran peptides in a dedicated database (AMPad) [13]. We used non-homologous sequences (less than 70% pair-wise identity amongst themselves) as a training set to correlate numerous physicochemical properties to this quantitative activity data, so as to develop an effective algorithm for predicting SI. The algorithm was successfully verified against another set of anuran peptides of known activity from AMPad, and was then implemented as a module of the ‘Designer’ tool, with associated rational sequence restrictions, to design novel AMP sequences predicted to have a high SI [13,14].

The choice of estimating SI values, rather than attempting to directly predict antimicrobial activity of designed AMPs, has several advantages. Selectivity index values are more sensitive to small changes in peptide sequence, so that one can more easily filter out descriptors with low relevance. Secondly, when relevant descriptors and data mining procedures are found, an enormous reduction in the number of potential AMPs can be achieved, and a workable load of lead candidates can be tested in dedicated experiments [14].

For example, amongst the  $8 \times 10^{29}$  possible sequences for a 23-residue peptide, the ‘Designer’ tool selected only seven [13]. It is based on two procedures, one to generate peptide sequences that are potentially amphipathic helices and have the characteristics of potent anuran AMPs, and the second to identify those with the highest predicted SI. Regarding the generation of peptide sequences, the analysis of those in the AMPad database allowed extracting mean and position-specific properties as well as motifs to guide the insertion of residues at each position, adding them in such a way that polar and non-polar amino acids remain separated correctly in a helical wheel projection. It restricts sequences to a net positive charge and mean hydrophobicity in a narrow range characteristic of the best anuran peptides (potent AMPs with  $SI > 20$ ). An amino acid selectivity index, derived from the same set of sequences, was applied to ensure a threshold number of those residues whose relative frequency is high in these peptides (E, D, Q, H, G). A motif regularity filter was also applied, based on regularity matrices for pairs of residues spaced  $i + 1$  and  $i + 4$  apart in the sequence [13]. Only at this stage were the sequences subjected to SI prediction.

The second procedure is based on our observation that the lengthwise distribution of residue hydrophobicities along a peptide sequence can affect its selectivity [15]. It results in a longitudinal component to the peptide’s amphipathicity, which we term the ‘sequence moment’

[13,14]. This is to be distinguished from Eisenberg’s ‘hydrophobic moment’ that considers the residue distribution around a helical wheel projection, as it is dependent on the sequence rather than the secondary structure. The sequence moment can be quantified by bending a sequence into a  $90^\circ$  arc and associating a hydrophobicity vector to each position, with the same origin as the coordinate system (small vectors in Fig. 1), and then calculating the vector sum (large vectors in Fig. 1). We found that the angle between sequence moments generated using two different scales correlated well with the peptide’s selectivity, and in particular between those calculated using the hydrophobicity scales of Guy [16] and Janin [17]. The final restriction on the generated sequences was thus that the predicted SI using these two scales has a value higher than a set threshold.

A first set of lead AMP candidates designed in this manner, with *E. coli* as reference microorganism, were named adeptantins (ADP1–7), an abbreviation for Automatically Designed Peptide Antibiotic Number 1–7. ADP1 (GICKHVGKALKGLKGLLGLGES-NH<sub>2</sub>) was previously tested and was found to be highly selective for Gram-negative bacteria, with MIC values 2–4  $\mu\text{M}$  against *E. coli* and 16  $\mu\text{M}$  against *Pseudomonas aeruginosa*, but over 128  $\mu\text{M}$  against *Staphylococcus aureus* [13]. It showed a remarkably low haemolytic activity ( $HC_{50} > 500 \mu\text{M}$ ), indicating that the training process used in our algorithm had successfully extracted the required selectivity attributes. This however needed to be confirmed for other lead adeptantins, and also related to the mode of action. To this end, in this paper we describe the functional and structural characterisation of two other adeptantins, and discuss these in relation to the confirmed high selectivity.

## 2. Materials and methods

### 2.1. Peptide selection

The Designer algorithm is described in detail in reference [13]. It proposed many 13 to 28 residue peptides predicted to have high SI values based on the analysis of sequence moments, but by applying restrictions to the primary sequences, structures and physicochemical properties, these were narrowed down to seven candidates. The Designer tool, as well as the AMPad database, can be downloaded from <http://sites.google.com/site/adeptantin1>. SI values can be calculated for any query sequence using the tool at <http://split4.pmfst.hr/split/dserv1/>.

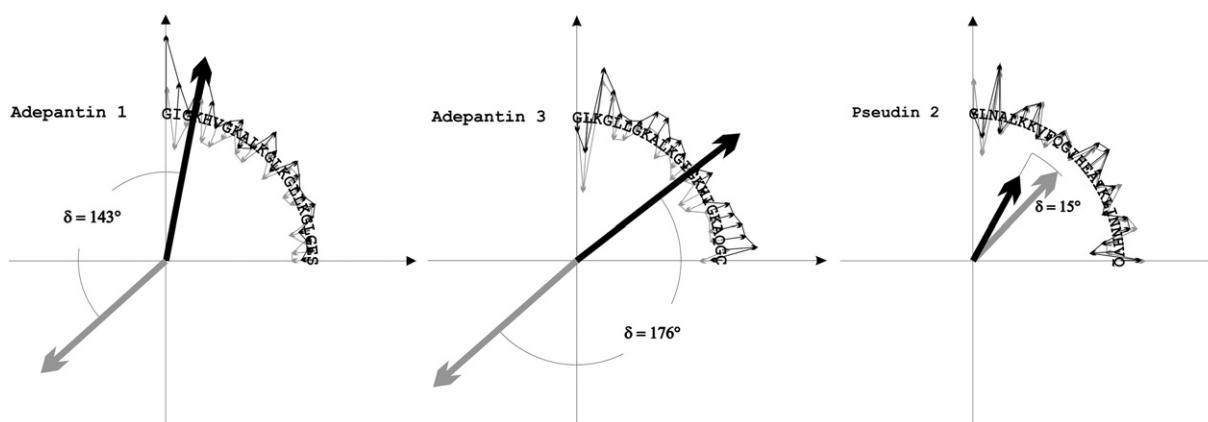


**Fig. 1.** Sequence moments for adeptantins 1 and 3 and the anuran peptide pseudin 2. For each peptide, the sequence is presented on an arc, and a smoothed hydrophobicity index is assigned to each position as represented by the small vector on this arc, having the same origin as the coordinate system. The smoothing procedure used to generate each index was based on a sliding window that takes into account the sequence environment about any given position, and which contracts near the peptide termini. Vectors in light grey and dark grey were generated using the scales of Guy [16] and Janin [17], respectively. The sum of the small vectors then results in the sequence moments shown as the large vectors centred on the origin. The angle between these vectors,  $\delta$ , correlates well with the selectivity indices of peptides in a database of natural anuran AMP sequences with published MIC (*E. coli*) and  $HC_{50}$  values (human RBC), and its cosine, can thus be used to predict the SI of similar artificially generated sequences. The scales of Guy and of Janin were previously found to give the best SI predictions for known anuran peptides, according to the linear, one-descriptor fit  $SI = 50.1 - 44.8 \times \cos(\delta)$  [13,14].

ADP1 was previously characterised [13], and ADP2 and ADP3 were respectively chosen as having the most and least similar primary sequence compared to ADP1 (Table 1). Both ADP2 and 3 carry a C-terminal cysteine by which they are amenable to covalent dimerisation or fluorescent labelling.

## 2.2. Peptide synthesis and characterisation

Peptides were synthesized as C-terminal amides on CEM Liberty automated microwave peptide synthesizer (CEM Corporation, Matthews, NC) using Fmoc-PAL-PEG-PS resin (substitution 0.34 mmol/g). Couplings were carried out with a fourfold excess of amino acids and PyBop as activator, at 75 °C in DMF. Preactivated Fmoc-Cys(-Trt)OPfp was used at 45 °C to reduce racemisation during the first C-terminal coupling. Fmoc deprotection was with 20% piperidine in DMF, whilst cleavage of peptide from the resin was performed with a trifluoroacetic acid (TFA), thioanisole, phenol, water, 3,6-dioxo-1,8-octanedithiol, triisopropylsilane mixture (83:3:2:2:8:2, v/v/v/v/v/v) for 3 h at room temperature. After cleavage, the peptides were precipitated in and repeatedly extracted with *t*-butyl methyl ether. Purification was carried out on a preparative reversed phase Waters RadialPak C18 column (21 mm × 150 mm, 5 µm, 300 Å), using a 20–55% gradient of acetonitrile in 70 min. Peptide purity was confirmed by ESI-MS on an Esquire 4000 mass spectrometer (Bruker Daltonics, Billerica, MA).

After lyophilisation, aliquots of adeptantins 2 and 3 were either acetamidated on the Cys residues, dimerised, or labelled with a fluorescent probe. Intermolecular disulfide bridge formation was achieved by suspending peptides in a water/DMSO (80:20) mixture at 6.5 pH for 48 h [18]. Peptide acetamidation and labelling with BODIPY-N-(2-aminoethyl)maleimide (BY) were performed as described [19,20]. After each procedure, the peptides were subjected to RP-HPLC and ESI-MS to verify the correct mass and purity and then they were repeatedly lyophilized from 10 mM HCl to remove TFA, before storage in the dark at –20 °C. Peptide concentrations of stock solutions were determined spectrophotometrically using the method of Waddell [21] as well as the calculated molar extinction coefficient at 214 nm [22]. For bodipylated peptides, the extinction coefficient of BODIPY was used [79,000 M<sup>-1</sup> cm<sup>-1</sup> at 504 nm in MeOH, Molecular Probes Handbook, Invitrogen, 10th Ed. p. 107].

## 2.3. Circular dichroism

CD spectroscopy was performed on a J-715 spectropolarimeter (Jasco, Tokyo, Japan) using 2 mm path length quartz cells and peptides (20 µM with respect to the peptide chains) in PBS 150 mM NaCl, 50% isopropanol (iPrOH) in SPB, 50% TFE in SPB and anionic or neutral liposomes (see below), to determine the peptides' propensity to interact with a membrane-like environment and to assume helical conformations. The helical content (% helicity) was estimated from

the molar ellipticity at 222 nm [23]. All displayed CD spectra are the accumulation of at least three scans.

## 2.4. Preparation of liposomes

Two types of LUVs (large unilamellar vesicles) were prepared as described in [24]. Briefly, dry anionic phosphatidylglycerol/diphosphatidylglycerol lipids (PG/dPG, 95:5 w/w) or neutral phosphatidylcholine/sphingomyelin/cholesterol lipids (PC/SM/Ch, 40:40:20 w/w) were dissolved in Chloroform/Methanol (2:1) solution, then evaporated using a dry nitrogen stream and vacuum-dried for 3 h. All lipids were from Sigma. The liposomes were resuspended in 1 ml of PBS to a concentration of 4 mM phospholipid and spun for 1 h at 40 °C. The vesicles were subjected to several freeze–thaw cycles before passing through a mini-extruder (Avanti Polar Lipids, Alabaster, AL) through successive polycarbonate filters with 1 µm, 0.4 µm and 0.1 µm pores. Final liposome concentrations were 0.4 mM phospholipid.

## 2.5. Bacterial cells and growth conditions

The antibacterial activity of the peptides was tested against the reference strains *E. coli* ATCC 25922, *S. aureus* ATCC 25923, *P. aeruginosa* ATCC 27853, *Salmonella typhimurium* ATCC 14028 and a clinical isolate of *Klebsiella pneumoniae*. *E. coli* ML-35 pYC strain was used for the outer- and inner-membrane permeabilisation assay [25]. To test for the barrier effect of the outer membrane, the *E. coli* BW 25113 (a K12 strain) was used with its deletion mutant  $\Delta waaP$  [26]. All the bacterial strains were stored at –80 °C and routinely grown onto Mueller Hinton (MH) agar plates (Oxoid, Cambridge, UK).

## 2.6. Antimicrobial activity assays

Minimum inhibitory concentration (MIC) values of the peptides were determined using a broth microdilution susceptibility test as previously described [27]. Briefly, serial two-fold dilutions of each peptide were prepared (final volume of 50 µl) in 96-well polypropylene microtiter plates (Sarstedt, Nümbrecht, Germany) with MH broth. Each dilution series included control wells without peptide. A total of 50 µl of the adjusted inoculum (approximately 5 × 10<sup>5</sup> cells/ml in MH broth) was added to each well. The MIC was taken as the lowest concentration of antimicrobial peptide resulting in the complete inhibition of visible growth after 18 h of incubation at 37 °C. Results are mean values of at least three independent determinations.

To determine the effects of peptides on bacterial growth kinetics, 200 µl suspensions of a mid-logarithmic bacterial culture (~1 × 10<sup>6</sup> cells/ml in MH broth) were placed in 96-well plates and incubated in a microplate reader (Tecan, Männedorf, Switzerland) at 37 °C, with periodic shaking, in the presence of different peptide concentrations [28]. The optical density (OD) at 620 nm was measured every 10 min for 4 h. IC<sub>50</sub> value was taken as the mean concentration of the peptide which inhibits bacterial growth by 50% at 210 min.

**Table 1**  
Sequences and physicochemical properties of designed adeptant peptides and natural anuran AMPs used for comparison.

Peptide	Amino acid sequence <sup>a</sup>	H <sup>b</sup>	µH <sub>rel</sub> <sup>b</sup>	δ <sup>c</sup>	D <sup>c</sup>	SI <sub>pred</sub> <sup>c</sup>
ADP1	GIGKHVKGKALKGLKGLLKGGLGES-NH <sub>2</sub>	–1.0	0.66	143°	–0.80	86
ADP2	GIGKHVKGKALKGLKGLLKGGLGEC-NH <sub>2</sub>	–0.9	0.66	156°	–0.91	91
ADP3	GLKGLLKGKALKGIGKHIGKAQGC-NH <sub>2</sub>	–1.1	0.51	176°	–1.00	95
Pseudin 2	GLNALKKVFQGIHEAIKLIINNHHVQ-NH <sub>2</sub>	–0.5	0.58	15°	0.97	7
Ascaphin 1	GFRDVLKGAAKAFVKTVAGHIAN-NH <sub>2</sub>	–1.1	0.43	95°	–0.08	54

<sup>a</sup> Residues that vary in ADP2 and 3 with respect to ADP1 are underlined.

<sup>b</sup> H = mean per residue hydrophobicity, µH<sub>rel</sub> = mean relative hydrophobic moment (relative amphipathicity), as calculated using the HydroMCalc applet (<http://www.bbcm.univ.trieste.it/~tossi/HydroCalc/HydroMCalc.html>), not considering the amidated C-termini. The hydrophobic moment is relative to a perfectly amphipathic, 18-residue helical peptide.

<sup>c</sup> δ = sequence moment angle (see Fig. 1), SI<sub>pred</sub> = predicted selectivity index, based on the D-descriptor value (cosδ), as estimated using the applet at <http://split4.pmfst.hr/split/dserv1/>.

**Table 2**  
Structural characteristics of tested adeptant peptides.

Peptide <sup>a</sup>	Charge <sup>b</sup>	MW <sup>calc</sup>	MW <sup>meas</sup>	% helical conformation <sup>d</sup>			
				H <sub>2</sub> O	TFE	LUV <sup>PG</sup>	LUV <sup>PC</sup>
ADP1	5	2259.0	2259.7	<5	35	55	<10
ADP2	5	2275.8	2275.4	–	–	–	–
ADP2(BY)	5	2689.8	2689.6	(<5) <sup>e</sup>	(40)	(50)	(<10)
ADP2(AM)	5	2332.9	2332.4	<5	45	60	<5
[ADP2] <sub>2</sub>	10	4549.6	4549.3	<5	40	50	<10
ADP3	6	2246.8	2246.5	–	–	–	–
ADP3(BY)	6	2660.8	2660.5	(<5) <sup>e</sup>	(55)	(50)	(<5)
ADP3(AM)	6	2303.8	2303.3	<5	30	53	<10
[ADP3] <sub>2</sub>	12	4491.5	4491.5	<5	40	45	<10

<sup>a</sup> ADP2 and 3 were not used as such, but either acetamidated at the C-terminal cysteine residue (AM), labelled with BODIPY maleimide at this residue (BY), or dimerised [ADP]<sub>2</sub>.

<sup>b</sup> Includes the N-terminus and considers histidine to be neutral.

<sup>c</sup> Calculated using the Peptide Companion software, measured with ESI-MS.

<sup>d</sup> Percent helicity determined according to Reed and Reed [23], using 20 μM helix in aqueous solution, 50% trifluoroethanol (TFE), anionic LUV<sup>PG</sup> (phosphatidylglycerol/diphosphatidylglycerol; 95:5) and neutral LUV<sup>PC</sup> (phosphatidylcholine/sphingomyelin/cholesterol; 2:2:1) in SPB buffer. Ellipticity was normalised per residue to take dimerisation into account.

<sup>e</sup> Not corrected for the presence of the BODIPY chromophore.

Minimal bactericidal concentration (MBC) assay was performed following MIC assay. At the end of MIC assay 10 μl aliquots of the medium were taken from peptide-containing wells with no visible bacterial growth. These were plated on MH agar, incubated for 24 h to allow colony growth. Peptide concentration causing at least a 99.9% reduction of the number of bacteria present at the beginning of MIC assay was defined as MBC value [29].

## 2.7. Bacterial membrane permeabilisation assays

The permeabilisation of the outer membrane of *E. coli* by the peptides was evaluated by following the unmasking of the periplasmic hydrolytic enzyme β-lactamase, using extracellular CENTA® as substrate [30], whilst that of the cytoplasmic membrane by unmasking cytoplasmic β-galactosidase activity using extracellular o-nitrophenyl-β-D-galactopyranoside (Gal-ONp) as substrate, as described previously [25,15]. The hydrolysis of both chromogenic substrates was monitored at 405 nm on a microplate reader. The β-galactosidase constitutive, lactose-permease deficient *E. coli* ML-35 pYC strain was used (~10<sup>7</sup> cells/ml bacteria), in the presence of 0.5 μM peptide and 0.15 mM CENTA or 0.25 μM peptide and 1.5 mM Gal-ONp in PBS.

Cytoplasmic membrane permeabilisation was also determined by flow cytometry, measuring propidium iodide (PI) uptake by bacterial cells [31]. A mid-logarithmic culture of *E. coli* ATCC 25922, diluted to 1 × 10<sup>6</sup> cells/ml, was incubated in MH broth with 0.25 μM peptides at 37 °C for different times. PI (Sigma-Aldrich, St Louis, MO) was then added to the peptide-treated bacteria at a final concentration of 10 μg/ml, and the cells were analysed in a FC500 flow cytometer (Beckman Coulter, Lexington, MA) after the given incubation times. Data analysis was performed with the FCS Express3 software (De Novo Software, Los Angeles, CA) and results are expressed as percentage of PI-positive cells.

## 2.8. Cytotoxic activity

The haemolytic activity of the peptides was determined by monitoring the release of haemoglobin at 405 nm using freshly isolated human red blood cells from healthy donors. Aliquots of 0.5%

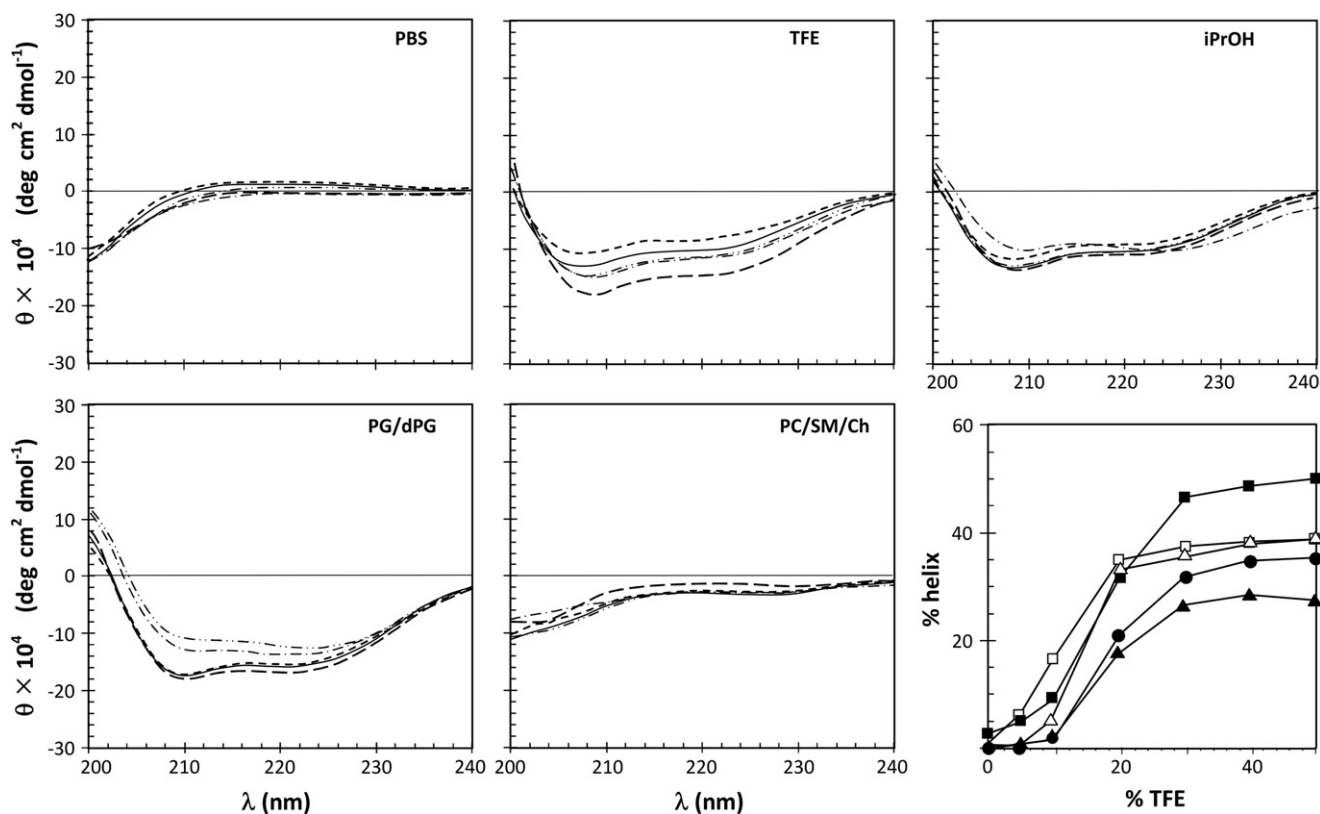


**Fig. 2.** Structure of adeptantins in different environments. CD spectra of peptides (20 μM of peptide chain) measured in phosphate buffered saline (PBS, pH7.4), 50% isopropanol (iPrOH), 50% trifluoroethanol (TFE), 1:1 phosphatidylglycerol/diphosphatidylglycerol LUVs in PBS (PG/dPG) or 2:2:1 phosphatidylcholine/sphingomyelin/cholesterol LUVs in PBS (PC/SM/Ch). The bottom right panel shows % helix with increasing TFE {ADP1 (—, —●—), ADP2 (---, —■—), ADP3 (- - -, —▲-), [ADP2]<sub>2</sub> (- · - · -, —□-) or [ADP3]<sub>2</sub> (- · - · - · -, —△-)}.

**Table 3**  
Antimicrobial and cytotoxic activities of adeptant peptides.

Peptide	MIC ( $\mu\text{M}$ ) <sup>a</sup>					MBC ( $\mu\text{M}$ ) <sup>b</sup>	IC <sub>50</sub> ( $\mu\text{M}$ ) <sup>c</sup>	HC <sub>50</sub> ( $\mu\text{M}$ ) <sup>d</sup>	SI <sup>e</sup>
	<i>E. coli</i> ATCC 25922	<i>S. aureus</i> ATCC 25923	<i>P. aeruginosa</i> ATCC 27853	<i>S. typhimurium</i> ATCC 14028	<i>K. pneumoniae</i> (ci)	<i>E. coli</i> ATCC 25922	<i>E. coli</i> ATCC 25922	RBC	
ADP1	2–4	> 128	16	–	–	4	1.5 ± 0.3	480 ± 60	190 ± 90
ADP2(AM)	1	> 128	32	16–32	64	2	0.8 ± 0.1	400 ± 100	400 ± 100
[ADP2] <sub>2</sub>	0.5–1	128	2	1	1	2	0.2 ± 0.05	16 ± 4	16 ± 4
ADP3(AM)	4	> 128	–	–	–	8	2.3 ± 0.3	> 500	> 125
[ADP3] <sub>2</sub>	0.5	64–128	–	–	–	0.5–1	0.2 ± 0.05	20 ± 4	40 ± 8

<sup>a</sup> Carried out in 100% (v/v) MH broth using  $5 \times 10^5$  cells/ml bacteria in the logarithmic phase—mean of at least 3 independent determinations carried out in duplicate.

<sup>b</sup> Concentration resulting in no bacterial growth, 2 independent determinations carried out in duplicate.

<sup>c</sup> Concentration resulting in 50% inhibition of growth, as calculated from data shown in Fig. 3B.

<sup>d</sup> Concentration resulting in 50% haemolysis of red blood cells (0.5% v/v) determined from data shown in Fig. 4.

<sup>e</sup> Selectivity index calculated as HC<sub>50</sub>/MIC for *E. coli*.

erythrocyte suspension in PBS done three times in triplicate, were incubated with different peptide concentrations, varying from 5  $\mu\text{M}$  to 500  $\mu\text{M}$ , at 37 °C for 30 min. 100% haemolysis was determined by

addition of Triton X-100 (0.2% final concentration). HC<sub>50</sub> value was taken as the mean concentration of the peptide causing 50% haemolysis.

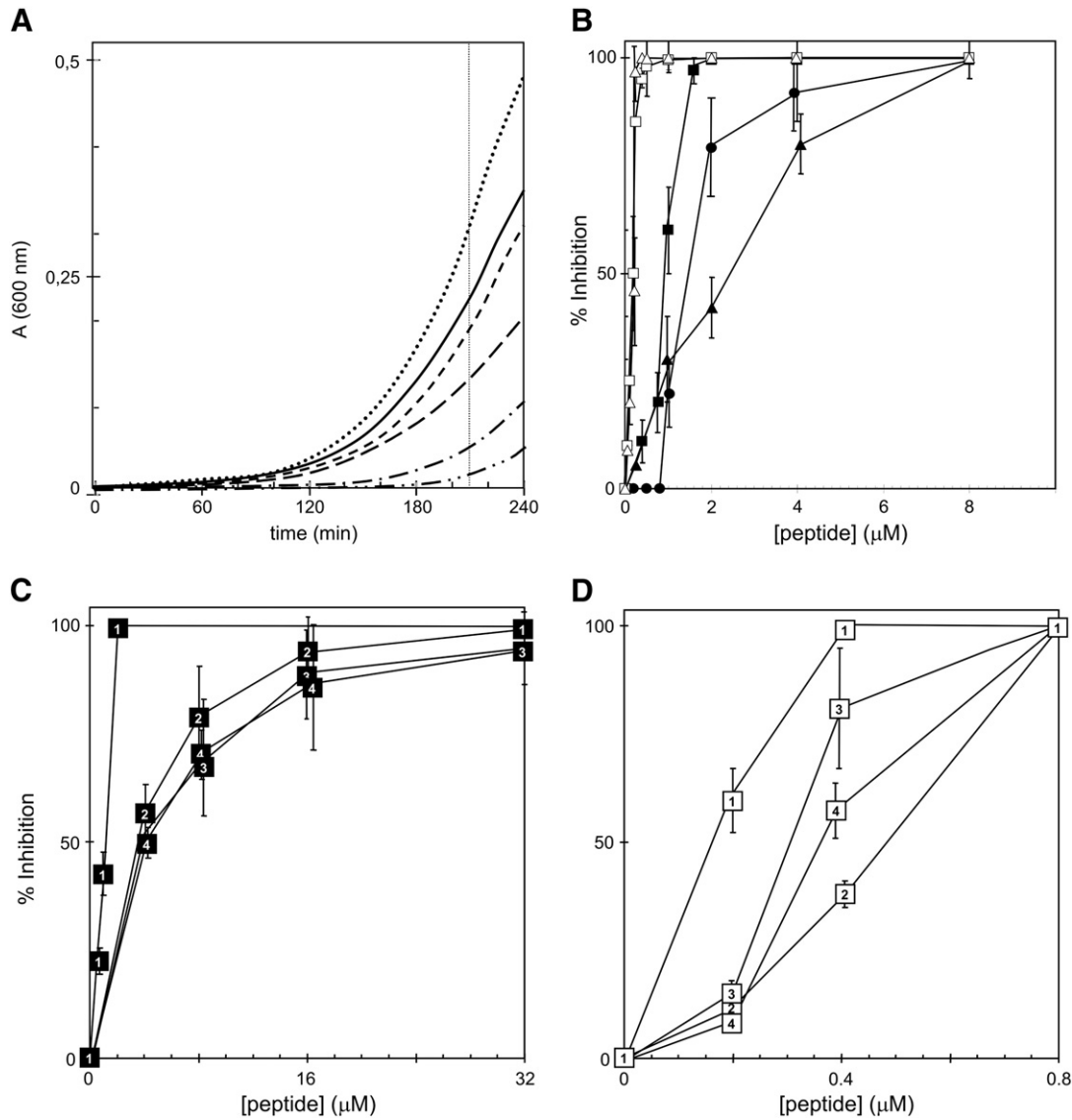


**Fig. 3.** Effect of peptides on bacterial growth kinetics. A) *E. coli* growth kinetics curves in the absence of peptides (·····) and in the presence of adeptants with peptide concentrations of 1  $\mu\text{M}$  for ADP1, ADP2(AM), ADP3(AM) and 0.5  $\mu\text{M}$  for dimers; B) % inhibition determined from the growth curves at 210 min ADP1 (—, ●), ADP2 (---, ■), ADP3 (---, ▲), [ADP2]<sub>2</sub> (---, □) or [ADP3]<sub>2</sub> (---, △); C) Effect of ADP2 and D) effect of [ADP2]<sub>2</sub> on the growth kinetics of *E. coli* (1), *P. aeruginosa* (2), *K. pneumoniae* (3) and *S. typhimurium* (4). These curves allowed the determination of the IC<sub>50</sub> values shown in Table 3. The error bars were determined from the results of three experiments carried out in triplicate.

U937 human monocytic cells at  $10^6$  cells/ml were incubated with BODIPY-labelled peptides (0.1 and 1  $\mu\text{M}$ ) and treated with PI for 5 min at room temperature. Membrane interaction and membrane permeabilisation were determined by flow cytometry by respectively monitoring fluorescence at 525 nm (BODIPY) and 610 nm (PI) at 5, 15 and 30 min, after which the treated cells were incubated with 0.1% trypan blue (TB) quencher, to distinguish between surface bound peptide (quenched) and internalised peptide (unquenched).

### 3. Results and discussion

#### 3.1. Peptide design and structural characterisation

A series of peptide sequences predicted to have high selectivity index values for activity with respect to Gram-negative bacteria was generated using the Designer algorithm [13,14]. One of these, adeptant 1 (ADP1), was functionally characterised and confirmed to have a high selectivity for Gram-negative bacteria with respect to blood cells. Two more peptides from the series, ADP2 and ADP3 (Table 1) were prepared to further confirm the efficacy of the Designer tool. Structurally, ADP2 is very similar to ADP1, but contains a C-terminal cysteine instead of serine, whilst ADP3 is only 35% identical, also bearing a C-terminal cysteine. This residue allows anchoring of a fluorescent probe, useful for studying membrane interactions and internalisation into cells. It also permits formation of covalent dimers, so as to probe the effects of aggregation. In the monomeric form, it was iodoacetamidated to prevent artefacts due to the reactivity of the sulfhydryl group.

The Designer algorithm used the lengthwise asymmetry of residue hydrophobicities to predict the SI, as briefly described in the introduction [13,14]. The smoothed hydrophobicity profiles and sequence moments for ADP-1 and -3 are shown in Fig. 1. The conversion of a peptide's smoothed hydrophobicity profile into a single sequence moment vector is a drastic reduction of the information contained by the profile, but appears to preserve the lengthwise asymmetry information relevant to the peptide's biological activity. This observation led to the choice of the best pair of hydrophobicity scales to use in this context (those of Guy [16] and of Janin [17]) and to the cosine of the angle between corresponding sequence moments as being the simplest quantitative structure–activity parameter having a good correlation with the SI.

Fig. 1 illustrates this concept by comparing ADP1, ADP3 with pseudin-2. The latter peptide, with  $\delta = 15^\circ$ , has a low predicted selectivity ( $SI_{\text{pred}} = 7$ , Table 1), and in fact has a very mediocre measured  $SI = 6$  [13]. ADP1 and ADP3, with  $\delta = 143^\circ$  ( $SI_{\text{pred}} = 86$ ) and  $\delta = 176^\circ$  ( $SI_{\text{pred}} = 95$ ) respectively, were predicted to be much more selective, and this had been experimentally verified for ADP-1 ( $SI = 200$  [13]). Note that the linear, one-descriptor fit is limited between allowable  $SI_{\text{pred}}$  values of 5.3 and 94.9, so that the closer the predicted value is to the higher limit, as is the case for ADP-2 and -3 (Table 1), the higher the experimental SI value is likely to be, and it could in fact be well above this value.

The peptides were synthesized in good yields ( $\geq 90\%$ ) and split into aliquots for different types of handling. To test the activity of monomeric peptides, the reactive sulfhydryl groups of the C-terminal cysteine residue were iodoacetamidated to avoid reaction with medium components. The resulting modified side chain may have hydrophobicity characteristics similar to those of glutamine. BODIPY (BY) was chosen to fluorescently label the peptide at the C-terminal cysteine, as it is stable, strongly fluorescent and unlike FITC, uncharged. It enabled us to follow the peptides' interaction with microbial and host cells. Covalent dimerisation required formation of an intermolecular disulphide bridge. Since AMPs often function by aggregating at the membrane surface, which affects both antimicrobial activity and cytotoxicity to host cell membranes, it allowed us to probe this effect. The correct structure and quality of all peptides were confirmed using analytical RP-HPLC coupled with ESI-MS (Table 2).

CD spectroscopy was used to study conformational properties of adeptantins in different environments. In water or aqueous buffers all peptides were substantially random coil (Table 2). In the presence of organic solvents such as 50% trifluoroethanol (TFE) or isopropanol (iPrOH) they undergo a transition to a helical conformation with different propensities (Fig. 2, Table 2). Determination of the percent helicity in a 5%–50% TFE range indicated that the transition was effectively complete at  $\geq 30\%$  TFE (Fig. 2). Covalent dimerisation did not markedly affect either the intensity or shape of the spectra with respect to the monomers, so that helix stacking did not appear to be relevant in the presence of helix-favouring solvent. Conversely, the shape, and in particular the  $\theta^{208}/\theta^{222}$  ratio of the spectra in the presence of anionic LUVs, suggested that the peptides may interact with these membranes in an aggregated helical form, and this was particularly evident with the covalently linked dimers. Both monomeric and dimeric peptides instead remained substantially as random coils in the presence of neutral LUVs, suggesting that they did not efficiently insert into this type of membrane.

#### 3.2. Antimicrobial activity

The antimicrobial activity of the peptides was assessed by determining both the minimum inhibitory concentration (MIC) and half maximal growth inhibitory concentration ( $IC_{50}$ ), against selected Gram-negative and Gram-positive bacteria (Table 3). In the MIC assay, the dimeric peptides were found to be more active against Gram-negative bacteria than the acetamidated monomeric versions.  $IC_{50}$  values obtained from bacterial growth inhibition assays (Fig. 3) confirmed these trends. It was significant that a single residue modification at the C-terminus (Ser in ADP1 to acetamidated Cys in ADP2(AM)) considerably affected activity. Furthermore, all peptides showed a lower potency against the Gram-positive *S. aureus*. This confirms that the activity of adeptantins in general is directed against Gram-negative bacteria. ADP2(AM) and its dimer were tested also against other Gram-negative microorganisms (Fig. 3C and D), and the monomer was somewhat less effective against *K. pneumoniae*, *S. typhimurium* or *P. aeruginosa* than against *E. coli*, the bacterial target used in the computational approach underlying the Designer algorithm, whilst the dimer showed a more potent, broad-spectrum activity. Determination of the minimal bactericidal concentration indicated that these peptides consistently have two-fold higher MBC than the MIC values (Table 3). Considering also the bacterial growth

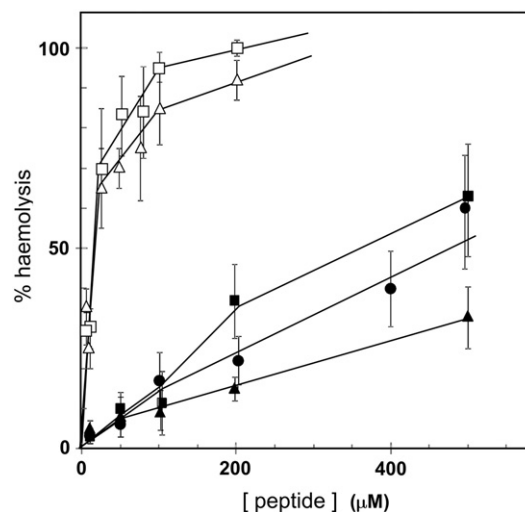


Fig. 4. Haemolytic activity of peptides. Erythrocytes 0.5% (v/v) were treated with increasing peptide concentrations (ADP1 —●—; ADP2 —■—; ADP3 —▲—; [ADP2]<sub>2</sub> —□—; [ADP3]<sub>2</sub> —△—). Error bars were determined from four experiments carried out in triplicate.

inhibition assays, it would thus appear that the peptides are bactericidal at a threshold concentration of between 1 and 8  $\mu\text{M}$ , depending on the peptide, whilst they are bacteriostatic at subtoxic concentrations.

### 3.3. Cytotoxic activity towards host cells

All three monomeric adeptantins were found to have very low haemolytic activities, assessed using 0.5% fresh human red blood cells (RBC) (Fig. 4) with comparably high  $\text{HC}_{50}$  values ( $>400 \mu\text{M}$ ), resulting in SI values  $>125$  (Table 3). The  $\text{HC}_{50}$  values were over an order of magnitude lower for dimeric ADP2 and 3, which displayed a significant toxicity at antimicrobial concentrations. CD spectra in the presence of neutral LUVs, mimicking host-cell membranes, do not indicate a high degree of helical structuring (Fig. 2), indicating that the peptides do not insert into this type of membrane. It may be that the dimeric peptides are capable of lysing host cells via a surface-type interaction. The different cytotoxicity of monomeric

and dimeric peptides suggests that peptide aggregation may be important in favouring this process.

To further probe the interaction of adeptantins with host cells, a flow cytometric study was carried out on U937 cells in the presence of fluorescently labelled ADP2-BY and ADP3-BY. By treating the cells with the impermeant quencher Trypan blue, it was possible to determine if peptide fluorescence was on the surface of the cells, or if some were internalised into the cytoplasm. By treating with PI, it was possible to probe whether the peptides induced membrane lysis at the concentrations used. In Fig. 5A–D, it can be seen that treatment with either of the fluorescently labelled adeptantins shifts the monoparametric peak to a considerably higher position, indicating that the peptides bind efficiently to the cell surface. They do so rapidly (within 5 min) and in a dose dependent manner up to 1  $\mu\text{M}$  (results not shown). Treating with the quencher efficiently reduces fluorescence, indicating that the peptides remain bound to the outside surface of the cells. Co-treatment of cells with PI showed that this occurs without subsequent membrane damage, as the signal shifts

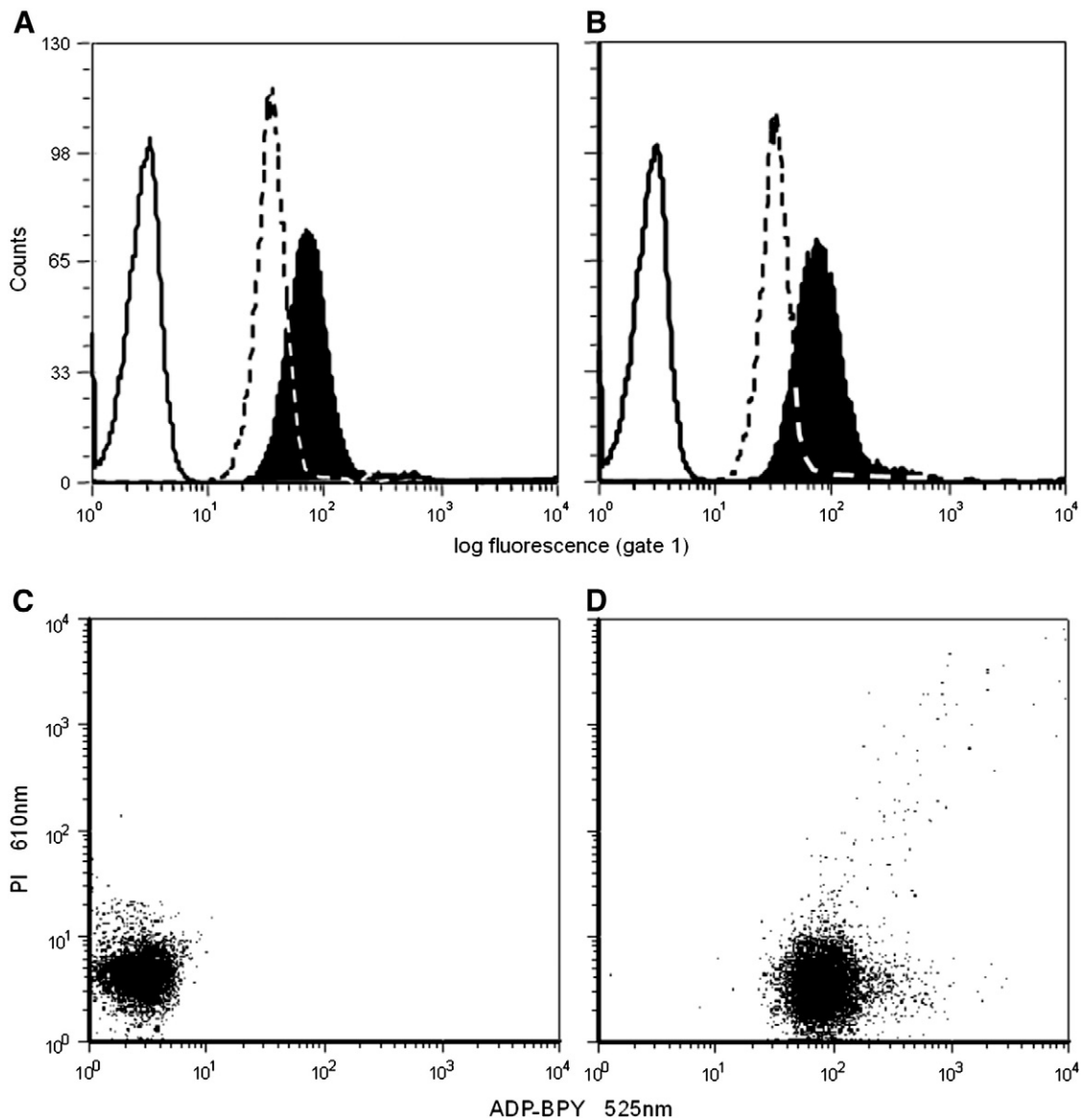


**Fig. 5.** Interaction of ADP2 and ADP3 with U937 cells. Monoparametric histograms for U937 cells in the absence (empty curves) and presence (filled curves) of ADP2-BY (A) and ADP3-BY (B), and with the impermeant, extracellular quencher Trypan blue also added (dashed line). Fluorescence dot plots for monocytes treated with PI and ADP2-BY (C) or ADP3-BY (D). Human leukemic monocytes (U937,  $10^6$  cells/ml) were incubated with BODIPY-labelled peptides (1  $\mu\text{M}$ ) for 30 min at room temperature before treating cells with Trypan blue or PI for 5 min, and then monitoring fluorescence at 525 nm (BODIPY) and 610 nm (PI) on the flow cytometer.

only on the 525 nm fluorescence axis (labelled peptide) and not on the 610 nm fluorescence axis (PI). These results confirm that the peptides interact with the surface of host cells, but are not cytotoxic at antimicrobial concentrations, in the monomeric form.

### 3.4. Interaction with bacterial membranes and permeabilisation

CD studies suggested an efficient insertion of adeptantins into anionic membranes (Fig. 2), which could initiate a process leading to membrane permeabilisation as part of their mode-of-action. Adeptantins are selective for Gram-negative bacteria, but they must first overcome the outer membrane barrier to reach and lyse the cytoplasmic membrane. To study the permeabilisation of both types of membranes, we used the *E. coli* ML-35 pYC strain, which constitutively produces both a cytoplasmic  $\beta$ -galactosidase and periplasmic  $\beta$ -lactamase. Damage to the outer membrane allows CENTA, a chromogenic substrate for the lactamase, to enter the periplasmic region, with an increased absorption at 405 nm. Damage to the cytoplasmic membrane allows Gal-ONp, a chromogenic substrate for the galactosidase, to reach this enzyme, also increasing absorption at 405 nm. Fig. 6A and B shows the hydrolysis curves for this strain when treated with the peptides in the presence of extracellular chromogenic substrates. Treatment with dimeric adeptantins results in a significantly faster hydrolysis of both substrates than the monomeric adeptantins, consistent with more

efficient membrane permeabilisation kinetics. Dimerisation seems to favour passage through both the outer membrane and permeabilisation of the cytoplasmic membrane, and this may be related to their greater potency.

To further test the barrier effect of the outer membrane, the activity of the peptides was tested against the *E. coli* BW 25113 strain (a K12 derived strain in which the LPS lacks the O-antigen polysaccharide), and a mutant of BW 25113 with an incompletely formed core saccharide so that the outer membrane is significantly destabilised. In *E. coli*, the *waa* locus contains several genes coding for enzymes involved in modification and assembly of the heptose region of the LPS core oligosaccharide, whose structure is critical for outer membrane stability. The  $\Delta waaP$  mutant, in which the *waaP* gene is deleted, lacks a kinase required for phosphorylation of the inner heptose in the core oligosaccharide, on which subsequent heptose additions and modifications depend. The LPS is destabilised and this results in hypersensitivity to antimicrobial agents, including peptides, a characteristic of deep-rough mutations [26].

In bacterial growth inhibition assays, the *E. coli* BW 25113 strain behaves similarly to the ATCC 25922 strain, with the monomers inhibiting growth in the order ADP2 > ADP1 > ADP3, and the dimers being much more effective than the monomers (Fig. 6C). The presence of the O-antigen polysaccharide thus does not seem to contribute to a barrier effect. The  $\Delta waaP$  deletion mutant shows a similar trend, with just a

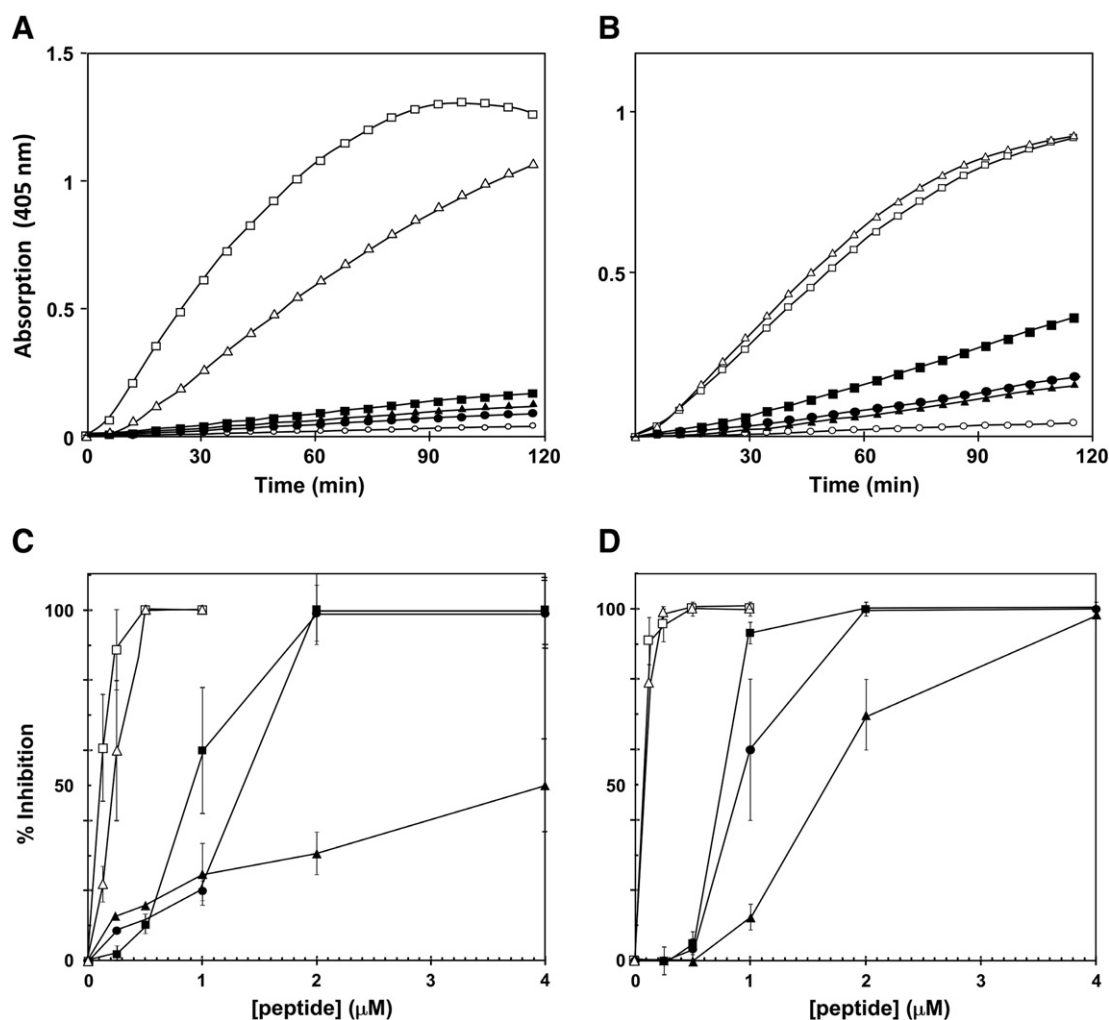


**Fig. 6.** Permeabilisation of the inner and outer membrane of *E. coli* ML-35 pYC by adeptantins and effect on bacterial growth kinetics. A) Permeabilisation of the cytoplasmic membrane determined by following the hydrolysis of the impermeant chromogenic substrate Gal-ONp by a cytoplasmic  $\beta$ -galactosidase; B) Permeabilisation of the outer membrane determined by following the hydrolysis of the impermeant chromogenic substrate CENTA® by the periplasmic enzyme  $\beta$ -lactamase; C) Effects of adeptantins on the growth kinetics of the *E. coli* BW 25113 strain; D) Effects of adeptantins on the growth kinetics of the *E. coli* BW 25113  $\Delta waaP$  strain; (no peptide —○—; ADP1 —●—; ADP2 —■—; ADP3 —▲—; [ADP2]<sub>2</sub> —□—; [ADP3]<sub>2</sub> —△—).

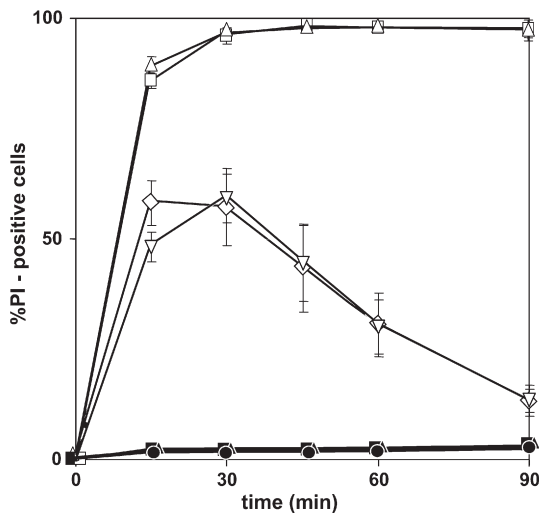


**Fig. 7.** Permeabilisation of *E. coli* ATCC 25922 to PI. Permeabilisation of the cytoplasmic membrane was determined by % of PI-positive bacterial cells by flow cytometric analyses. Bacteria at  $10^6$  cells/ml were treated with  $0.25 \mu\text{M}$  peptides before adding PI; (ADP1 —●—; ADP2 —■—; ADP3 —▲—; [ADP2]<sub>2</sub> —□—; [ADP3]<sub>2</sub> —△—). BODIPY-labelled ADP2 and ADP3 were also tested (ADP2-BY —○—; ADP3-BY —▽—).

slight increase in inhibition efficiency for all peptides (Fig. 6D). Taken together, these results indicate that the LPS layer of the outer membrane is not a significant barrier for adeptantins, in particular for the dimeric form.

Permeabilisation of the cytoplasmic membrane was further studied by monitoring the internalisation of PI into the *E. coli* ATCC 25922 strain. At the concentrations used ( $0.25 \mu\text{M}$ ), which are sub-toxic for the monomers, no permeabilisation was evident (Fig. 7), whilst for the dimers it was over 90% within 15 min, in agreement with both their increased antimicrobial activity and increased permeabilisation to Gal-ONp (Fig. 6A). Fluorescent labelling of monomeric peptides also appears to increase the permeabilisation of *E. coli* cells although this shows curious and as yet unexplained time dependence.

In conclusion, we have confirmed that the Designer algorithm is capable of elaborating AMPs that are highly selective for Gram-negative bacteria, and in particular *E. coli*, having very high selectivity indices. The exceptionally low cytotoxicity towards eukaryotic cells and inactivity against Gram-positive bacteria, suggest them as potentially useful tools for exploring selectivity mechanisms. A common characteristic of these short, linear AMPs is the capacity to adopt a helical structure in the presence of negatively charged membranes, which favours insertion into and permeabilisation of these, whilst they only appear to interact with the surface of neutral membranes. The fact that their sequences are particularly rich in glycine residues might have some significance in this respect. Furthermore, it appears that the capacity to dimerise plays a significant role in modulating both the antimicrobial activity and cytotoxicity towards host cells, as shown by covalently dimerised peptides. These results, apart from confirming the validity of our computational AMP design method, and setting the foundations for the design of further optimised variants that may be developed into useful anti-infective agents, bring some new insights into the mode of action of the numerous and important class of amphipathic, helical AMPs.

## Acknowledgements

This work was partly supported by the Croatian Ministry of Science, Education and Sports, grant 177-1770495-0476, and the Friuli Venezia Giulia L26 project R3A2. N.I. acknowledges an Alpe Adria 2009 grant. We also acknowledge Prof. Dr. Damir Vukićević and Viktor Bojović for assistance in developing and sharing user friendly variations of the SI-estimator algorithms and Dr. Sabrina Pacor for assistance with cytotoxicity tests.

## References

- [1] G. Taubes, The bacteria fight back, *Science* 321 (2008) 356–361.
- [2] M. Zasloff, Antimicrobial peptides of multicellular organisms, *Nature* 415 (2002) 389–395.
- [3] M.R. Yeaman, N.Y. Yount, Unifying themes in host defence effector polypeptides, *Nat. Rev. Microbiol.* 5 (2007) 727–740.
- [4] L.T. Nguyen, E.F. Haney, H.J. Vogel, The expanding scope of antimicrobial peptide structures and their modes of action, *Trends Biotechnol.* 29 (2011) 464–472.
- [5] A. Peschel, H.G. Sahl, The co-evolution of host cationic antimicrobial peptides and microbial resistance, *Nat. Rev. Microbiol.* 4 (2006) 529–536.
- [6] A. Yeung, S. Gellatly, R. Hancock, Multifunctional cationic host defence peptides and their clinical applications, *Cell. Mol. Life Sci.* 68 (2011) 2161–2176.
- [7] R. Hammami, I. Fliss, Current trends in antimicrobial agent research: chemo- and bioinformatics approaches, *Drug Discov. Today* 15 (2010) 540–546.
- [8] A. Tossi, L. Sandri, A. Giangaspero, Amphipathic, alpha-helical antimicrobial peptides, *Biopolymers* 55 (2000) 4–30.
- [9] M. Dathe, H. Nikolenko, J. Meyer, M. Beyersmann, M. Bienert, Optimization of the antimicrobial activity of magainin peptides by modification of charge, *FEBS Lett.* 501 (2001) 146–150.
- [10] I. Zelezetsky, A. Tossi, Alpha-helical antimicrobial peptides—using a sequence template to guide structure–activity relationship studies, *Biochim. Biophys. Acta* 1758 (2006) 1436–1449.
- [11] O. Taboureau, O.H. Olsen, J.D. Nielsen, D. Raventos, P.H. Mygind, H.H. Kristensen, Design of novispirin antimicrobial peptides by quantitative structure–activity relationship, *Chem. Biol. Drug Des.* 68 (2006) 48–57.
- [12] Y. Huang, J. Huang, Y. Chen, Alpha-helical cationic antimicrobial peptides: relationships of structure and function, *Protein Cell* 1 (2010) 143–152.
- [13] D. Juretic, D. Vukicevic, N. Ilic, N. Antcheva, A. Tossi, Computational design of highly selective antimicrobial peptides, *J. Chem. Inf. Model.* 49 (2009) 2873–2882.
- [14] D. Juretic, D. Vukicevic, D. Petrov, M. Novkovic, V. Bojovic, B. Lucic, N. Ilic, A. Tossi, Knowledge-based computational methods for identifying or designing novel, non-homologous antimicrobial peptides, *Eur. Biophys. J.* 40 (2011) 371–385.
- [15] I. Zelezetsky, S. Pacor, U. Pag, N. Papo, Y. Shai, H.G. Sahl, A. Tossi, Controlled alteration of the shape and conformational stability of alpha-helical cell-lytic peptides: effect on mode of action and cell specificity, *Biochem. J.* 390 (2005) 177–188.
- [16] H.R. Guy, Amino acid side-chain partition energies and distribution of residues in soluble proteins, *Biophys. J.* 47 (1985) 61–70.
- [17] J. Janin, Surface and inside volumes in globular proteins, *Nature* 277 (1979) 491–492.
- [18] J.P. Tam, C.R. Wu, W. Liu, J.W. Zhang, Disulfide bond formation in peptides by dimethyl sulfoxide. Scope and applications, *J. Am. Chem. Soc.* 113 (1991) 6657–6662.
- [19] T. Creighton, Disulfide bonds between cysteine residues, in: W. Gray (Ed.), *Protein Structure: A Practical Approach*, Oxford University Press, New York, 2002, pp. 165–186.
- [20] M. Scocchi, M. Mattiuzzo, M. Benincasa, N. Antcheva, A. Tossi, R. Gennaro, Investigating the mode of action of proline-rich antimicrobial peptides using a genetic approach: a tool to identify new bacterial targets amenable to the design of novel antibiotics, *Methods Mol. Biol.* 494 (2008) 161–176.
- [21] W.J. Waddell, A simple ultraviolet spectrophotometric method for the determination of protein, *J. Lab. Clin. Med.* 48 (1956) 311–314.
- [22] B.J. Kuipers, H. Gruppen, Prediction of molar extinction coefficients of proteins and peptides using UV absorption of the constituent amino acids at 214 nm to enable quantitative reverse phase high-performance liquid chromatography-mass spectrometry analysis, *J. Agric. Food Chem.* 55 (2007) 5445–5451.
- [23] J. Reed, T.A. Reed, A set of constructed type spectra for the practical estimation of peptide secondary structure from circular dichroism, *Anal. Biochem.* 254 (1997) 36–40.
- [24] F. Morgera, L. Vaccari, N. Antcheva, D. Scaini, S. Pacor, A. Tossi, Primate cathelicidin orthologues display different structures and membrane interactions, *Biochem. J.* 417 (2009) 727–735.
- [25] E. Tiozzo, G. Rocco, A. Tossi, D. Romeo, Wide-spectrum antibiotic activity of synthetic, amphipathic peptides, *Biochem. Biophys. Res. Commun.* 249 (1998) 202–206.
- [26] J.A. Yethon, D.E. Heinrichs, M.A. Monteiro, M.B. Perry, C. Whitfield, Involvement of waaY, waaQ, and waaP in the modification of *Escherichia coli* lipopolysaccharide and their role in the formation of a stable outer membrane, *J. Biol. Chem.* 273 (1998) 26310–26316.
- [27] M. Benincasa, M. Scocchi, E. Podda, B. Skerlavaj, L. Dolzani, R. Gennaro, Antimicrobial activity of Bac7 fragments against drug-resistant clinical isolates, *Peptides* 25 (2004) 2055–2061.
- [28] M. Mattiuzzo, A. Bandiera, R. Gennaro, M. Benincasa, S. Pacor, N. Antcheva, M. Scocchi, Role of the *Escherichia coli* SbmA in the antimicrobial activity of proline-rich peptides, *Mol. Microbiol.* 66 (2007) 151–163.
- [29] A. Tossi, M. Scocchi, B. Skerlavaj, R. Gennaro, Identification and characterization of a primary antibacterial domain in CAP1 8, a lipopolysaccharide binding protein from rabbit leukocytes, *FEBS Lett.* 339 (1994) 108–112.
- [30] R.N. Jones, H.W. Wilson, W.J. Novick Jr., A.L. Barry, C. Thornsberry, In vitro evaluation of CENTA, a new beta-lactamase-susceptible chromogenic cephalosporin reagent, *J. Clin. Microbiol.* 15 (1982) 954–958.
- [31] E. Podda, M. Benincasa, S. Pacor, F. Micali, M. Mattiuzzo, R. Gennaro, M. Scocchi, Dual mode of action of Bac7, a proline-rich antibacterial peptide, *Biochim. Biophys. Acta* 1760 (2006) 1732–1740.